

# Image reconstruction from limited Fourier data

Hsin M. Shieh

Department of Electrical Engineering, Feng Chia University, 100 Wenhwa Road, Seatwen, Taichung, Taiwan 40724

Charles L. Byrne

Department of Mathematical Sciences, University of Massachusetts Lowell, One University Avenue, Lowell, Massachusetts 01854

Received February 6, 2006; revised May 3, 2006; accepted May 18, 2006; posted May 26, 2006 (Doc. ID 67763)

We consider the problem of reconstructing a function  $f$  with bounded support  $S$  from finitely many values of its Fourier transform  $F$ . Although  $f$  cannot be band limited since it has bounded support, it is typically the case that  $f$  can be modeled as the restriction to  $S$  of a  $\sigma$ -band-limited function, say  $g$ . Our reconstruction method is based on such a model for  $f$ . Of particular interest is the effect of the choice of  $\sigma > 0$  on the resolution. © 2006 Optical Society of America

OCIS codes: 100.3010, 100.3020, 100.3190, 100.6640.

## 1. INTRODUCTION

Image reconstruction in many fields, such as x-ray diffraction, electron microscopy, and diffraction optics, can be interpreted as the problem of estimating a function from its Fourier-transform values. While there has been considerable effort in the development of algorithms, this problem has generally proved to be difficult. Mathematically, reconstructing a real function (i.e., object energy) from a finite number of Fourier values leads to an infinite number of potential solutions. To single out one particular data-consistent solution, one can require that some functional of the image, such as its entropy, be optimized,<sup>1-3</sup> or that the solution be closest to some other appropriate prior estimate according to a given distance criterion.<sup>4-7</sup> For some applications the main requirement may be that the reconstruction algorithm be easily implemented and rapidly calculated. Best results are achieved when the criteria chosen force the reconstructed image to incorporate features of the true function that are known *a priori*, such as support limitation.

In this paper we are concerned with the reconstruction from finitely many Fourier-transform values of a function  $f(x)$  with bounded support region  $S$ . The variable  $x$  may be multidimensional. We assume that  $f(x)$  can be approximated by the restriction to  $S$  of a function  $g(x)$  whose Fourier transform  $G(\omega)$  is zero for  $|\omega| > \sigma$ ; that is,  $f(x)$  is the restriction to  $S$  of a  $\sigma$ -band-limited function.

The paper is organized as follows. Section 2 introduces the theory behind the reconstruction algorithm using the notation of the one-dimensional problem. In Section 3 we extend this algorithm to the two-dimensional problem. The new algorithm is then applied to one-dimensional and two-dimensional simulations.

## 2. MATHEMATICAL BACKGROUND

Suppose that  $N$  Fourier-transform data sampled at frequencies  $\omega_n$ , for  $n = 1, 2, \dots, N$ , are represented as

$$F(\omega_n) = \int_{-\infty}^{\infty} f(x) \exp(-jx\omega_n) dx, \quad (1)$$

for  $n = 1, 2, \dots, N$ . In many applications,  $f(x)$  can be support limited to some region  $S$ , and it is typically the case that this function  $f(x)$  can be well modeled as the restriction to  $S$  of a function, say

$$g(x) = \sum_{n=1}^N a_n h_n(x). \quad (2)$$

$h_n(x)$ , for  $n = 1, 2, \dots, N$ , are basis functions. For simplicity, we define  $S$  to be  $|x| \leq \tau$ . Here, we shall take the sinc function,  $\sin[\sigma(x-x_n)]/[\sigma(x-x_n)]$ , as  $h_n(x)$ . Although  $f(x)$  itself cannot be band limited since it is support limited, we take as our estimate of  $f(x)$  the data-consistent function of the form

$$\hat{f}(x) = \sum_{n=1}^N a_n \frac{\sin[\sigma(x-x_n)]}{\sigma(x-x_n)}, \quad (3)$$

for  $|x| \leq \tau$ . To force  $\hat{f}(x)$  to be data consistent, that is, for

$$\hat{F}(\omega_m) = F(\omega_m), \quad \text{for } m = 1, 2, \dots, N, \quad (4)$$

we must have

$$F(\omega_m) = \sum_{n=1}^N a_n A_{mn} \quad (5)$$

with

$$A_{mn} = \int_{-\tau}^{\tau} \frac{\sin[\sigma(x-x_n)]}{\sigma(x-x_n)} \exp(-jx\omega_m) dx. \quad (6)$$

The reconstruction procedure is to solve Eq. (5) for the coefficients  $a_n$ , for  $n = 1, 2, \dots, N$ , and then substitute these coefficients into Eq. (3).

To obtain accurate reconstruction using the algorithm

in Eq. (3) for realistic applications, *a priori* knowledge about the true support domain where the object function  $f(x)$  resides is helpful, and an appropriate choice for  $\sigma, x_1, x_2, \dots, x_N$  is also necessary. While one may argue that lack of specific knowledge of the true support domain is typically the case, the expected support domain in the reconstruction must be large enough to accommodate the true object function  $f(x)$  at least. A high-resolution reconstructed image typically requires a tight estimate of the true support; choosing a wide support typically gives an image similar to the discrete Fourier transform (DFT) estimate. The existence of object energy outside the expected support leads to errors, because  $\hat{f}(x)$  is necessarily data consistent and requires some artifact energy in the expected support to compensate for object energy discarded by the expected support.

Let  $\sigma$  and  $\{x_1, x_2, \dots, x_N\}$  represent the basis functions' parameters and spatial shifts, respectively. The larger  $\sigma$  is, the narrower the shape of the basis functions. Choosing a larger value of  $\sigma$  has a greater potential in recovering finer features, whereas a good reconstruction also depends on the locations of  $\{x_1, x_2, \dots, x_N\}$  as well as the profile of the true object function  $f(x)$ . Placing the  $\{x_1, x_2, \dots, x_N\}$  at uniform intervals is generally good; concentrating them either inside or outside the true support is not recommended. In addition, the interval  $\Delta x_n = x_{n+1}$

$-x_n$  for  $n=1, 2, \dots, N-1$  should not be an integer multiple of  $\pi/\sigma$ , since zeros of basis functions will coincide in the sense that  $\Delta x_n = m\pi/\sigma$  ( $m \in \mathbb{Z}$ ). A high-quality image is typically obtained by taking a great diversity of spatial shifts of basis functions, which typically means, in turn, that the region spanned by  $\{x_1, x_2, \dots, x_N\}$  should be wide.

To test our developed algorithm, we applied it to computed Fourier data in which 17 data samples were taken at unit-interval frequencies accessible with low-pass filtering ( $\{\omega_1, \omega_2, \dots, \omega_{17}\} = \{-8, \dots, 8\}$ ). The function  $f(x)$  being reconstructed (the solid curve) and having its support in the range  $[-\pi/4, \pi/4]$  and the DFT estimate (the dotted curve) are shown in Fig. 1. We apply the algorithm in Eq. (3) with the points of  $\{x_1, x_2, \dots, x_{17}\}$  positioned at a constant interval. Some representative examples with different expected support domains are shown in Figs. 2–5, for which each takes  $\sigma$  as  $\Omega=8$  (the largest value of  $|\omega_n|$  for  $n=1, 2, \dots, 17$ ), and different locations for the  $\{x_1, \dots, x_N\}$  are chosen.

Compared with the DFT estimate in Fig. 1, superior resolution can be seen in Figs. 3 and 4, where the choices of  $\tau=2$  and  $\tau=1$ , respectively, are used. Comparable results in Fig. 2 are obtained when we use  $\tau=\pi$  (too large) and poorer results in Fig. 6 when we use  $\tau=0.7$  (too small). Positioning all the points of  $\{x_1, x_2, \dots, x_{17}\}$  outside the true support is usually not a good choice, as clearly seen in Figs. 2(f) and 3(f). On the other hand, setting all the points inside the true support could provide an acceptable resolution, but not a very good one typically, as seen in Figs. 2(e), 3(e), and 4(e).

Appropriately increasing the value of  $\sigma$  larger than  $\Omega$  can typically improve the image resolution, especially for the case in which the region where the  $\{x_1, x_2, \dots, x_{17}\}$  reside is not wide. If choosing larger values of  $\sigma$  than  $\Omega$  for the examples in Figs. 4(a)–4(d), the corresponding results are shown in Figs. 6(a)–6(d), from which the most significant improvement can be clearly seen in part (d). This is because a greater diversity of the basis function's profile

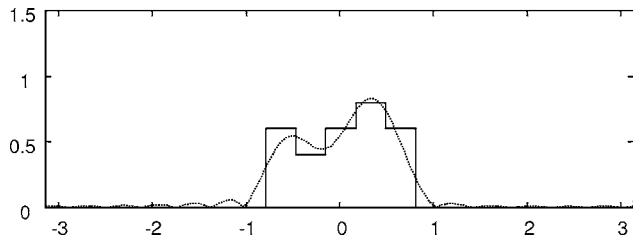


Fig. 1. DFT estimate from 17 computed Fourier data sampled at frequencies  $\{-8, \dots, 8\}$ .

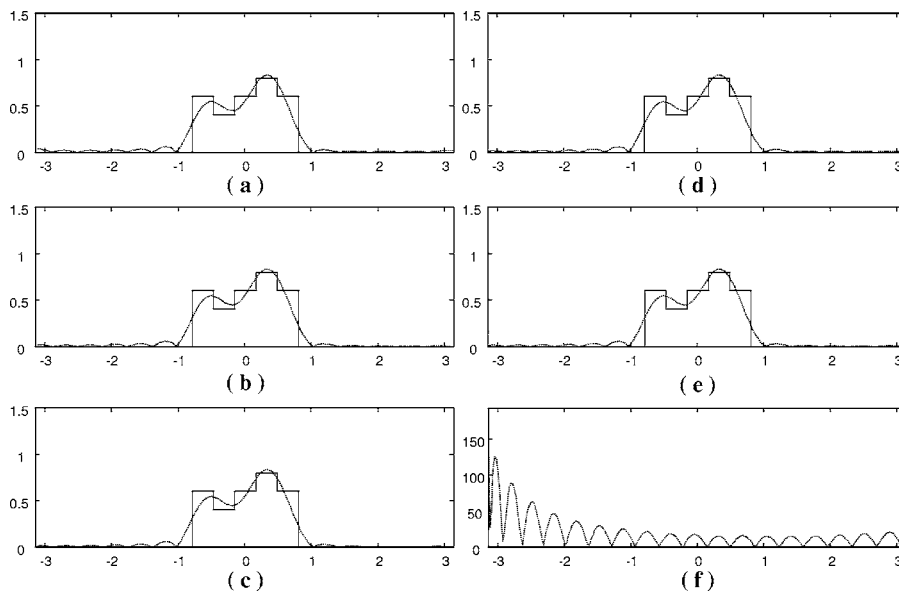


Fig. 2. Estimate by Eq. (3) with  $\tau=\pi$ ,  $\sigma=8$ , and  $\{x_1, x_2, \dots, x_{17}\}$  sampled at a constant interval over the ranges (a)  $[-3, 3]$ , (b)  $[-2, 2]$ , (c)  $[-1, 1]$ , (d)  $[-\pi/4, \pi/4]$ , (e)  $[-0.6, 0.6]$ , (f)  $[-3, -1]$ . In each case the condition number of the matrix  $A$  in Eq. (5) is 2.968,  $1.680 \times 10^4$ ,  $6.382 \times 10^9$ ,  $4.059 \times 10^{11}$ ,  $3.846 \times 10^{13}$ ,  $1.208 \times 10^{13}$ .

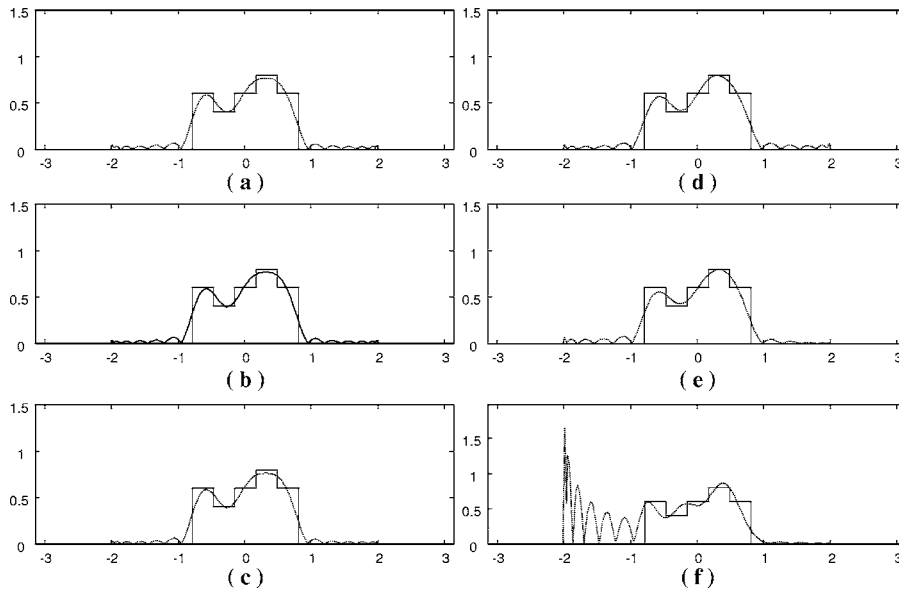


Fig. 3. Same as Fig. 2 but with  $\tau=2$  and the condition number of the matrix A in Eq. (5) as (a)  $1.441 \times 10^7$ , (b)  $4.119 \times 10^{10}$ , (c)  $1.204 \times 10^{16}$ , (d)  $1.393 \times 10^{16}$ , (e)  $5.624 \times 10^{16}$ , and (f)  $1.286 \times 10^{16}$ .

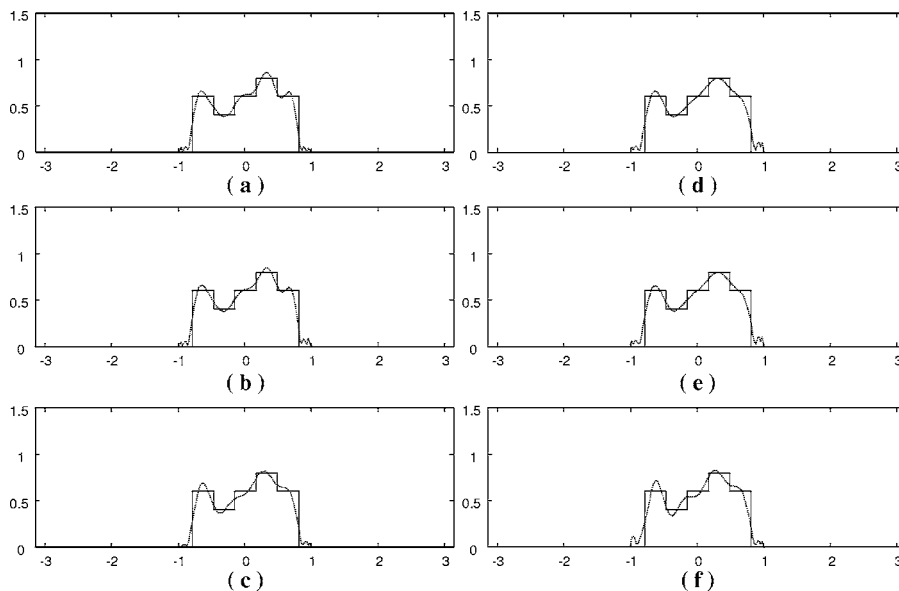


Fig. 4. Same as Fig. 2 but with  $\tau=1$  and the condition number of the matrix A in Eq. (5) as (a)  $7.730 \times 10^{16}$ , (b)  $3.479 \times 10^{16}$ , (c)  $7.162 \times 10^{16}$ , (d)  $3.961 \times 10^{16}$ , (e)  $5.301 \times 10^{16}$ , (f)  $2.514 \times 10^{17}$ .

used in the reconstruction can be extended by narrowing its period of zeros ( $\pi/\sigma$ ), equivalently increasing the value of  $\sigma$ .

For each simulation it is typically the case that the matrix A in Eq. (5) is ill-conditioned, as the condition numbers show in Figs. 2–6. Although the condition number for each example in this paper does not cause a problem for an accurate image, it is recommended to use the regularization method for noisy data in practical applications. It is easy to improve the condition number by regularization, such as in the Miller–Tikhonov sense, when the data set is not large. For large problems an iterative method, such as the algebraic reconstruction technique, can be applied to solve the system.

### 3. TWO-DIMENSIONAL IMAGING PROBLEM

Consider the reconstruction of a two-dimensional function  $f(x,y)$  from the Fourier values at frequencies  $(\alpha_n, \beta_n)$  for  $n = 1, 2, \dots, N$ :

$$F(\alpha_n, \beta_n) = \int_{-\infty}^{\infty} \int_{-\infty}^{\infty} f(x,y) \exp(-jx\alpha_n - jy\beta_n) dx dy. \quad (7)$$

Let  $f(x,y)$  be bounded and its support region  $S$  defined by  $|x| \leq \tau_x, |y| \leq \tau_y$ . In a manner similar to the one-dimensional case, the reconstruction algorithm we consider is based on a model of  $f(x,y)$  as the restriction to  $S$  of a band limited function. The estimate is then

$$\hat{f}(x,y) = \sum_{n=1}^N a_n \frac{\sin[\sigma_\alpha(x-x_n)]}{\sigma_\alpha(x-x_n)} \frac{\sin[\sigma_\beta(y-y_n)]}{\sigma_\beta(y-y_n)}, \quad (8)$$

for  $|x| \leq \tau_x$ ,  $|y| \leq \tau_y$ . In Eq. (8), the coefficients  $a_n$  for  $n = 1, 2, \dots, N$  will satisfy

$$F(\alpha_m, \beta_m) = \sum_{n=1}^N a_n A_{mn} B_{mn} \quad (9)$$

with

$$A_{mn} = \int_{-\tau_x}^{\tau_x} \frac{\sin[\sigma_\alpha(x-x_n)]}{\sigma_\alpha(x-x_n)} \exp(-jx\alpha_m) dx \quad (10)$$

and

$$B_{mn} = \int_{-\tau_y}^{\tau_y} \frac{\sin[\sigma_\beta(y-y_n)]}{\sigma_\beta(y-y_n)} \exp(-jy\beta_m) dy. \quad (11)$$

The integrals in Eqs. (10) and (11) can be computed in terms of the sine integral and cosine integral functions. The sine integral function is defined for  $-\infty < x < \infty$  by<sup>8</sup>

$$Si(x) = \int_x^\infty \frac{\sin(t)}{t} dt, \quad (12)$$

and the cosine integral function is defined for  $0 < x < \infty$  by

$$Ci(x) = \int_x^\infty \frac{\cos(t)}{t} dt. \quad (13)$$

By changing variables and using the trigonometric identities, the definition of  $A_{mn}$  in Eq. (10) can be equivalently written as

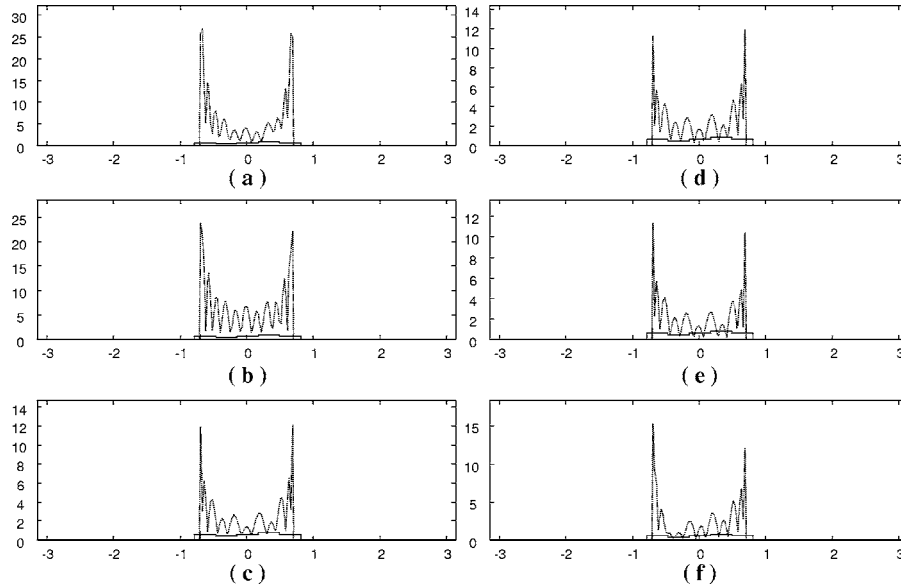


Fig. 5. Same as Fig. 2 but with  $\tau=0.7$  and the condition number of the matrix  $A$  in Eq. (5) as (a)  $7.402 \times 10^{17}$ , (b)  $7.684 \times 10^{16}$ , (c)  $5.695 \times 10^{16}$ , (d)  $9.364 \times 10^{16}$ , (e)  $1.575 \times 10^{17}$ , and (f)  $2.109 \times 10^{17}$ .

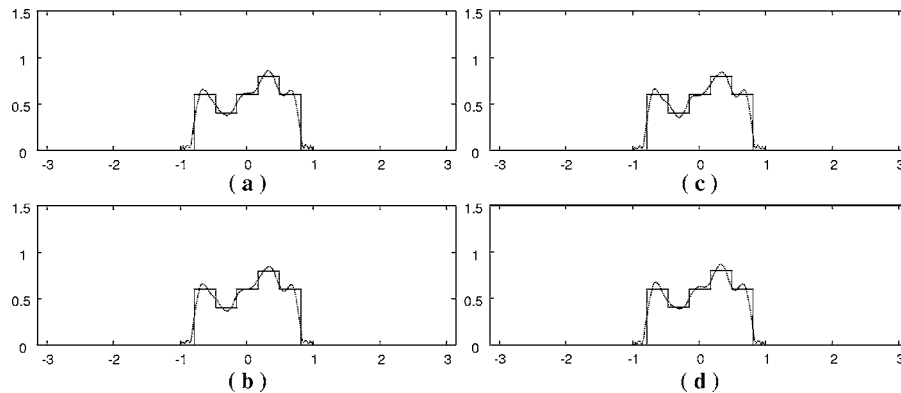


Fig. 6. Estimate by Eq. (3) with  $\tau=1$  and (a)  $\sigma=13$  with  $\{x_1, x_2, \dots, x_{17}\}$  sampled at a constant interval over the range  $[-3, 3]$ , (b)  $\sigma=17$  with  $\{x_1, x_2, \dots, x_{17}\}$  over the range  $[-2, 2]$ , (c)  $\sigma=18$  and  $\{x_1, x_2, \dots, x_{17}\}$  over the range  $[-1, 1]$ , (d)  $\sigma=13$  and  $\{x_1, x_2, \dots, x_{17}\}$  over the range  $[-\pi/4, \pi/4]$ . In each case the condition number of the matrix  $A$  in Eq. (5) is  $5.931 \times 10^{14}$ ,  $3.024 \times 10^{12}$ ,  $2.055 \times 10^{14}$ ,  $1.830 \times 10^{16}$ , respectively.

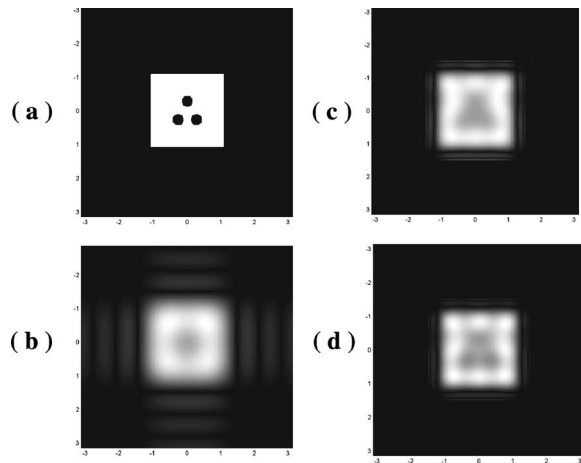


Fig. 7. Reconstruction of a two-dimensional function from its limited Fourier values with (a) the object function, (b) the DFT estimate, (c) the estimate by Eq. (8) with  $\tau_x = \tau_y = 1.5$ ,  $\sigma_\alpha = \sigma_\beta = 4$ , and  $\{(x_n, y_n) | n = 1, 2, \dots, 81\}$  sampled on a regular grid over the range  $-3 \leq x \leq 3$ ,  $-3 \leq y \leq 3$ , (d) the same as (c) but with  $\sigma_\alpha = \sigma_\beta = 6$ .

$$\begin{aligned}
 A_{mn} &= D \int_{-\tau_x}^{\tau_x} \frac{\sin[\sigma_\alpha(x - x_n)]}{\pi(x - x_n)} \exp[-j(x - x_n)\alpha_m] dx \\
 &= \frac{D}{2\pi} [Si(h_1) - Si(h_2) + Si(h_3) - Si(h_4)] \\
 &\quad + \frac{jD}{2\pi} [Ci(h_1) - Ci(h_2) - Ci(h_3) + Ci(h_4)], \quad (14)
 \end{aligned}$$

where  $D = \pi \exp(-j\alpha_m x_n) / \sigma_\alpha$ ,  $h_1 = (\sigma_\alpha + \alpha_m)(-\tau_x - x_n)$ ,  $h_2 = (\sigma_\alpha + \alpha_m)(\tau_x - x_n)$ ,  $h_3 = (\sigma_\alpha - \alpha_m)(-\tau_x - x_n)$ , and  $h_4 = (\sigma_\alpha - \alpha_m)(\tau_x - x_n)$ . The evaluation of  $B_{mn}$  can be done in similar fashion.

To illustrate the algorithm for two-dimensional imaging applications, we simulate an example of reconstructing a two-dimensional function from its Fourier values ( $9 \times 9$  low-pass data). In Fig. 7, the resolution of the estimate by Eq. (8) is clearly superior to the DFT estimate by making good choices of  $\sigma_\alpha$ ,  $\sigma_\beta$ ,  $\tau_x$ ,  $\tau_y$ , and  $\{(x_n, y_n) | n = 1, 2, \dots, 81\}$ .

#### 4. CONCLUSIONS

Our algorithm models the function to be reconstructed as the restriction to a finite domain of a  $\sigma$ -band-limited function. Having chosen the form of the estimate as the superposition of such band-limited functions, the coefficients are chosen so as to satisfy consistency with the finitely many Fourier-transform data values. The algorithm involves the selection of several parameters, such as the width  $\tau$  of the true support of the function, the degree  $\sigma$  of band limitation, and the center points for the several sinc functions that appear in the superposition model. We

have seen that the  $\tau$  should accommodate the true support at least, in order to produce an acceptable reconstruction or better. The resolution can be improved as the  $\sigma$  increases, allowing us to overcome, to a degree, the limitations imposed by the finite data. If we take  $\sigma$  too large, the sinc functions centered at the points  $x_n$  will have main lobes that are essentially disjoint; in the limit, as  $\sigma$  goes to infinity, the reconstructed image will consist of delta functions supported at the  $x_n$ . This suggests that, in future work, we may want to consider nonuniformly distributed points  $x_n$  and values of  $\sigma$  that are allowed to vary with  $n$ . This will allow us to concentrate higher resolution where needed. One possible application of this approach could be to reducing the partial-volume effect in emission tomography.<sup>9</sup>

Our discussion here has focused on Fourier data, but that is not essential. We have left the issue of sensitivity to noise for future work, apart from noting that choosing  $\tau$  too small causes the reconstruction to fail.

#### ACKNOWLEDGMENTS

The work of C. Byrne was supported in part by the National Institute of Biomedical Imaging and Bioengineering, under grants R01EB001457 and R01EB002798. The views expressed here do not necessarily reflect those of the funder.

The e-mail address for H. M. Shieh is hmshieh@fcu.edu.tw.

#### REFERENCES

1. J. P. Burg, "Maximum entropy spectral analysis," presented at The 37th Annual Meeting of the Society of Exploration Geophysicists (Oklahoma City, Oklahoma, 1967).
2. J. P. Burg, "The relationship between maximum entropy spectra and maximum likelihood spectra," *Geophysics* **37**, 375–376 (1972).
3. C. L. Byrne, *Signal Processing: A Mathematical Approach* (AK Peters, Ltd., 2005).
4. C. L. Byrne and R. M. Fitzgerald, "Reconstruction from partial information, with application to tomography," *SIAM J. Appl. Math.* **42**, 933–940 (1982).
5. C. L. Byrne and R. M. Fitzgerald, "Spectral estimators that extend the maximum entropy and maximum likelihood methods," *SIAM J. Appl. Math.* **44**, 425–442 (1984).
6. C. L. Byrne and M. A. Fiddy, "Estimation of continuous object distributions from limited Fourier magnitude measurements," *J. Opt. Soc. Am. A* **4**, 112–117 (1987).
7. H. M. Shieh, C. L. Byrne, and M. A. Fiddy, "Image reconstruction: a unifying model for resolution enhancement and data extrapolation. Tutorial," *J. Opt. Soc. Am. A* **23**, 258–266 (2006).
8. D. Widder, *Advanced Calculus* (Dover, 1989).
9. P. Pretorius, M. King, T.-S. Pan, D. deVries, S. Glick, and C. Byrne, "Reducing the influence of the partial volume effect on SPECT activity quantitation with 3D modeling of spatial resolution in iterative reconstruction," *Phys. Med. Biol.* **43**, 407–420 (1998).